AIMS Mathematics, 9(3): 6850–6877.
DOI: 10.3934/math.2024334
Received: 09 December 2023
Revised: 19 January 2024
Accepted: 29 January 2024
Published: 19 February 2024

http://www.aimspress.com/journal/Math

Research article

Modeling and diagnosis Parkinson disease by using hand drawing: deep learning model

Theyazn H. H. Aldhyani[1,2,*], Abdullah H. Al-Nefaie[1,3] and Deepika Koundal[1,4]

[1] King Salman Center for Disability Research, Riyadh 11614, Saudi Arabia
[2] Applied College in Abqaiq, King Faisal University, P.O. Box 400, Al-Ahsa 31982, Saudi Arabia
[3] Department of Quantitative Methods, School of Business, King Faisal University, Saudi Arabia
[4] School of Computer Science, University of Petroleum & Energy Studies, Dehradun, India

* **Correspondence:** Email: taldhyani@kfu.edu.sa.

Abstract: Patients with Parkinson's disease (PD) often manifest motor dysfunction symptoms, including tremors and stiffness. The presence of these symptoms may significantly impact the handwriting and sketching abilities of individuals during the initial phases of the condition. Currently, the diagnosis of PD depends on several clinical investigations conducted inside a hospital setting. One potential approach for facilitating the early identification of PD within home settings involves the use of hand-written drawings inside an automated PD detection system for recognition purposes. In this study, the PD Spiral Drawings public dataset was used for the investigation and diagnosis of PD. The experiments were conducted alongside a comparative analysis using 204 spiral and wave PD drawings. This study contributes by conducting deep learning models, namely DenseNet201 and VGG16, to detect PD. The empirical findings indicate that the DenseNet201 model attained a classification accuracy of 94% when trained on spiral drawing images. Moreover, the model exhibited a receiver operating characteristic (ROC) value of 99%. When comparing the performance of the VGG16 model, it was observed that it attained a better accuracy of 90% and exhibited a ROC value of 98% when trained on wave images. The comparative findings indicate that the outcomes of the proposed PD system are superior to existing PD systems using the same dataset. The proposed system is a very promising technological approach that has the potential to aid physicians in delivering objective and dependable diagnoses of diseases. This is achieved by leveraging important and distinctive characteristics extracted from spiral and wave drawings associated with PD.

Keywords: modeling and predicting Parkinson's disease; deep learning, artificial intelligence;

diagnosis; drawing images
Mathematics Subject Classification: 11Y40, 11Y16, 68T10, 68Q32

1. Introduction

Parkinson's disease (PD) is a neurodegenerative disorder that is defined by the progressive degeneration of the nervous system, which leads to the manifestation of symptoms such as tremors, stiffness, and bradykinesia [1]. The aforementioned condition is a neurodegenerative disorder characterized by the progressive deterioration of brain function. PD is associated with a range of consequences, including cognitive impairment, mood disturbances such as sadness, dysphagia, mastication difficulties, sleep disturbances or restlessness, and urinary and gastrointestinal dysfunction. PD significantly impacts an individual's everyday motor functions, particularly their automatic movements. This neurodegenerative disorder impairs one's capacity to execute involuntary actions, such as smiling or blinking. In addition, the impairment of bodily appendages has been documented in a variety of instances attributed to PD.

The likelihood of having PD is elevated amongst the elderly population. The fact that it affects 1% of the overall elderly population is a cause for concern [2]. Furthermore, PD poses a significant risk to the elderly population, making elder care facilities the most likely setting for encountering individuals affected by this condition.

According to a study conducted by the World Health Organization in 2019, over 8.5 million individuals were diagnosed with PD [3]. The incidence of this ailment is positively correlated with an advancing age, as shown by the fact that only 4% of affected individuals are below the age of 50. Globally, PD is of the most prevalent neurodegenerative diseases, comes in second after Alzheimer's disease, and impacts millions of individuals [4,5]. Now, physicians are limited in addressing the symptoms of this disorder due to the nascent stage of therapy [6]. The diagnosis of this ailment is not definitively established and is mostly dependent on the patient's medical history [3]. Due to the high costs and time requirements associated with an invasive diagnosis and therapy, it is imperative to develop a straightforward and dependable approach to diagnosing this illness [7,8].

In relation to nonmotor manifestations shown by individuals with PD, a diverse array of symptoms may be observed, including mood disorders and depressive states. These symptoms may be represented in the patient's facial expressions [9], such as language and other relevant factors [8,10]. The main primary objective of this research is to use handwriting modeling techniques, spirals, and waves to assess the impact of PD on both motor and nonmotor functions, while addressing the lack of research on the topic of employing both drawing spirals and waves while having PD.

The use of deep learning (DL) models has brought about a significant transformation within the domain of biomedical and medical image analyses [11]. DL models have been used in several fields, such as segmentation, detection, and disease classification [12]. DL models have a remarkable ability to extract high-level characteristics, thus resulting in an improved accuracy during disease classification. This may be largely attributed to their exceptional capacity for generalization. Furthermore, convolutional neural networks (CNNs) have played a vital role in facilitating the advancement of medical image processing. CNNs have shown significant achievements in several medical imaging applications [13–15].

Hence, it is essential to present a methodology that can extract the significant aspects that have a

crucial impact on the detection of PD. PD is characterized by its progressive nature and is a condition that gradually advances over time. Early detection of the illness offers an opportunity for effective management with appropriate medicine, perhaps leading to its eradication [16,17]. Figure 1 displays the symptoms of PD.

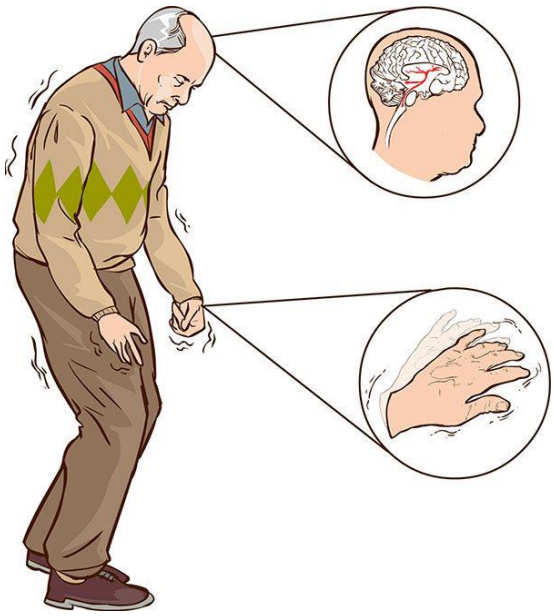

Figure 1. Symptoms of PD [17].

1.1. Contributions

This article presents a comprehensive account of the training and testing processes used for the DL models. Our primary objective was to construct a model capable of accurately diagnosing PD based on an analysis of spiral and wave drawings. This aspect is significant due to the propensity of older patients that experience rapid exhaustion, thus rendering it impractical to expect them to perform many sketching assignments within the confines of a primary care setting. Furthermore, from a clinical standpoint, it is noteworthy that we demonstrated the diagnostic potential of DL models in identifying PD. The DenseNet201 and VGG16 DL models have been notably efficacious in accurately differentiating persons with PD from healthy individuals by utilizing an analysis of spiral and wave drawing images. In this study, we conducted a comparative analysis between the outcomes of improved DL models and several current systems, as well as an open access code that used the same dataset. Our observations indicate that the proposed system exhibits a notable level of accuracy in the detection of PD when applied to two different drawings of images.

1.2. Background

PD has been identified by several researchers using DL techniques. The use of voice analyses, brain scans, and artistic depictions using meander patterns, spirals, waves, and similar elements has been employed as a diagnostic system [18]. Due to its high level of accuracy, DL models are often used in the field of medical imaging for the early prediction of PD.

Rastegar et al. [19] introduced a novel model aimed at detecting PD. The methodology used involved the utilization of the random forest algorithm to analyze cytokine data. The examination of molecular data pertaining to cytokines provides significant insights into PD patients. The random forest approach was used alongside entropy and dataset data to diagnose Parkinson's illness. This system was evaluated using the root mean square error (RMSE).

Nilashi et al. [20] developed system based on the machine learning (ML) algorithm to predict PD using speech data. The University of California Irvine dataset was used to evaluate the system. The cluster technique was used to predict illnesses. The proposed model was evaluated using the RMSE metric, yielding a score of (RMSE=0.537) at the test dataset.

The use of neural networks and decision trees was proposed in a study to enhance the diagnostic process of PD [21]. Sharma et al. [22] used speech data as a medium to identify PD, and the Unified PD Scale served as the foundation for their detection approach. The support vector machines (SVM) method was applied to detect PD. The efficacy of learning models is notably impacted by the quality of the data. The use of data preparation strategies can augment the efficacy of learning models. A regression analysis was performed on the preprocessed data using the SVM method. The performance of the model was assessed by computing its RMSE, which yielded a value of 0.24. Chen et al. [23] introduced a DL model to forecast PD using speech data obtained from individuals diagnosed with the condition. Nooritawati et al. [24] used gait movement as a prediction metric for PD. The proposed model was used to extract and statistically represent gait variables pertaining to the spatiotemporal, kinematic, and kinetic aspects. The data that was not cleansed underwent a preprocessing step, which included both intra-group and inter-group normalization. The aforementioned preprocessing approaches were used to extract gait information related to the spatiotemporal, kinematic, and kinetic components. Moreover, an artificial neural network model was used to detect PD [25], which used a linear SVM approach for clinically diagnosed with PD and proposed a cost-effective technique for the early detection of PD [26]. The use of a deep multivariate voice data analysis (DMVDA) has been employed to detect and diagnose disorders via the implementation of deep learning classifiers [27]. Maachi et al. [28] proposed the development of a CNN known as 1D-Convnet to predict PD. Moreover, several research have used transfer learning methodologies [29–32]. The usefulness of several machine learning models, such as deep neural networks, SVMs, and CNNs, to predict PD has been examined [33–37]. Pereira et al. [36] used a recurrent neural network (RNN) to enhance the monitoring of PD. The prediction of PD development was conducted using speech data via a hybrid model that incorporated CNNs and long short-term memory (LSTM). The aforementioned methodology was used in a research investigation carried out by [31]. Vasquez et al. [32] aimed to diagnose PD using DL techniques, feature-extraction methods, and dataset-balancing procedures.

Talitckii et al. [33] used several machine learning techniques, including random forest, logistic regression, SVM, light gradient boosting machine (GBM), and a stacked ensemble model to discern PD from other neurological conditions that exhibit motor discrepancies, thereby leveraging the data collected from wearable sensors. The highest level of accuracy, reaching 85%, was attained while using both feature sets. However, when just the tremor characteristics were utilized as the input for the machine learning models, the accuracy decreased to 80%.

Pereira et al. [34] developed a dataset named "HandPD" by using handwriting examinations conducted on a sample of 74 individuals diagnosed with PD and 18 control persons. The training phase of Naive Bayes, Optimum-Path Forest, and SVM models included using around 90% of the dataset. Moreover, the researchers devised a CNN structure to categorize the "HandPD" dataset into two

distinct groups: PD and controls [35]. Additionally, meta-heuristic optimization methods were used to effectively adjust the hyperparameters. The researchers saw a notable increase in the classification accuracy, namely reaching 90%, when compared to their previous study [34]. Pereira et al. [36] proposed many CNN structures to categorize the handwriting dynamics acquired from a smart pen that was fitted with a set of sensors. The study used a sample of 224 individuals diagnosed with PD and 84 control participants. The CNN architectures were evaluated against the raw data categorized using baseline classification techniques.

Shaban et al. [37] investigated the use of a fine-tuned, pre-trained, VGG-19 model to distinguish between people diagnosed with PD and controls. The aforementioned discrimination was predicated upon the examination of datasets, including wave and spiral handwriting patterns. The model being evaluated showed a significant improvement in both the accuracy and sensitivity, exceeding 88% and 86%, respectively. Table 1 presents a complete overview of the latest breakthroughs in ML and DL approaches using different types of PD datasets.

Table 1. Summary of the states of the art ML and DL by using different types of PD datasets.

Authors, year	Types of datasets	Models	Object
Vanegas et al. [47], 2018	EGG dataset	LR, DT, Extra tree	Biomarkers PD
Oh et al. [48], 2018	EGG dataset	CNN	PD detection
Wagh et al. [49], 2020	EGG dataset	CNN	PD detection
Shi et al. [50], 2019	EGG dataset	CNN-RNN	PD detection
Zhang et al. [51], 2019	MRI dataset	ResNext model	Detecting prodnormal PD
Ramirez et al. [52], 2020	MRI dataset	Convolution auto encoder	Detecting de Novo PD
Prasuhn et al. [53], 2020	MRI dataset	SVM, MKL	PD detection
Rasheed et al. [54], 2020	Voice dataset	BPVAM	Detecting de Novo PD
Gunduz et al. [55], 2019	Speech dataset	GB,	PD detection
Moon et al. [56], 2020	Gait features dataset	ANN, SVM, KNN	Detecting ET versus PD
Zeng et al. [57], 2016	Gait features dataset	RBF	PD detection
Pdisher et al. [58], 2020	Sensory dataset	CNN	PD diagnosis
Taliki et al. [33], 2020	Sensory dataset	RF	Detecting ET versus PD
Shaban et al. [37], 2020	Handwriting dataset	VGG1-16	PD detection
Robin [59], 2020	Handwriting dataset (Same dataset)	RF, CNN, RestNet50	PD detection
Stpete_ishii [60], 2023	Handwriting dataset (Same dataset)	CNN	PD detection
Shaban et al. [61], 2020	Handwriting dataset (Same dataset)	CNN	PD detection
Adrian [62], 2019	Handwriting dataset (Same dataset)	CNN	PD detection

Wroge et al. [38] proposed a deep neural network-based approach to classify PD by utilizing the voices of patients. Dai et al. [39] designed U-net neural network algorithms to enhance the diagnosis of PD. Authors have applied various preprocessing approaches such as histogram equalization and gray level transformation to improve the U-net performance. The outcome data from preprocessing is processed using the U-net architecture. Rusz et al. [40] used a multilayer perceptron approach to detect several neurological illnesses, including PD. Haq et al. [41] designed a system to detect PD by analyzing the vocal characteristics of patients using preprocessing approaches to handle the missing and scaling of the data. The L_1-norm SVM approach was used to extract the features from the voices of patients; the k-fold cross-validation method was used to evaluate their proposed system. The proposed system achieved a high accuracy of 99%. Prince et al. [42] introduced a wearable sensor to detect Parkinson's disease when placed on the patient's body. The sensors were used to monitor the actions and vital signs of the person being examined, without the need for physically inspecting the individual.

Zeng et al. [43] used a radial basis function (RBF) to detect PD using a dataset that contained 93 individuals with PD and 73 healthy controls. The suggested approach achieved an accuracy rate of 96.7%.

Muniz et al. [44] proposed logistic regression, probabilistic neural network, and SVM approaches to diagnose PD. The authors used a ground reaction force (GRF) as the input for the system. Pfister et al. [45] used a CNN to categorize PD into three classes: On, Off, and dyskinesia. The dataset was generated from wearable sensors and included a total of 30 patients. Drotar et al. [46] used feature selection and SVM techniques to distinguish between 37 patients with PD and 38 control individuals based on their handwriting motions. The calculated accuracies of the system for in-air trajectories was determined to be 84%, while it was 78% for on-surface movements.

2. Materials and methods

Figure 2 presents the framework of the detection of PD. This work aims to propose the development of a system using artificial intelligence methods for the purpose of screening and staging PD, as well as identifying biomarkers of the condition via the analysis of handwriting examinations. The "HandPD" study demonstrated significant methods to detect PD at an early stage.

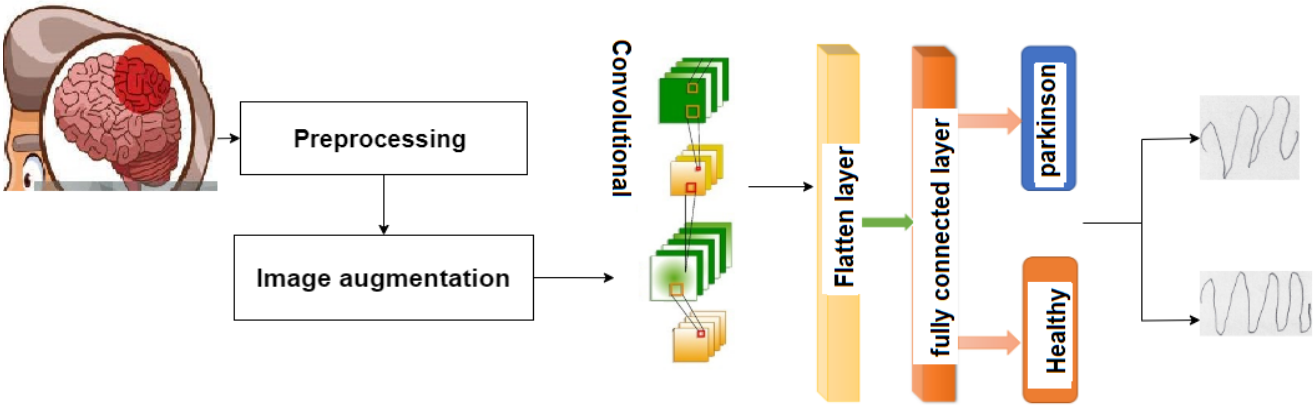

Figure 2. Proposed system for detecting PD.

2.1. Data acquisition

The dataset used in this study was developed by Adriano et al. [62] from the Innovation and Technology Assessment of the Federal University. The dataset was comprised of images that were pre-divided into a training set and a testing set. The training set included images of spirals and waves, as did the testing set. The study revealed that individuals diagnosed with PD had decreased drawing speeds and pen pressures, particularly among those in the more severe stages of the condition. The dataset consisted of a total of 204 images, including 102 images of spiral patterns and 102 images of waves. From this dataset, 70% of images were used for training purposes, while the remaining 30% of images were reserved for testing. The dataset consists of two distinct classes: individuals diagnosed with PD and healthy individuals. Figures 3 and 4 show a few samples of spiral and wave images.

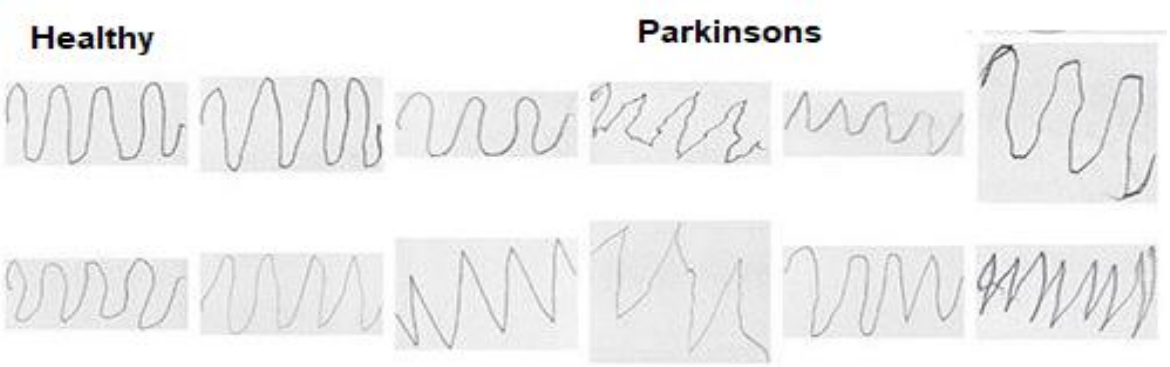

Figure 3. Samples of the wave images.

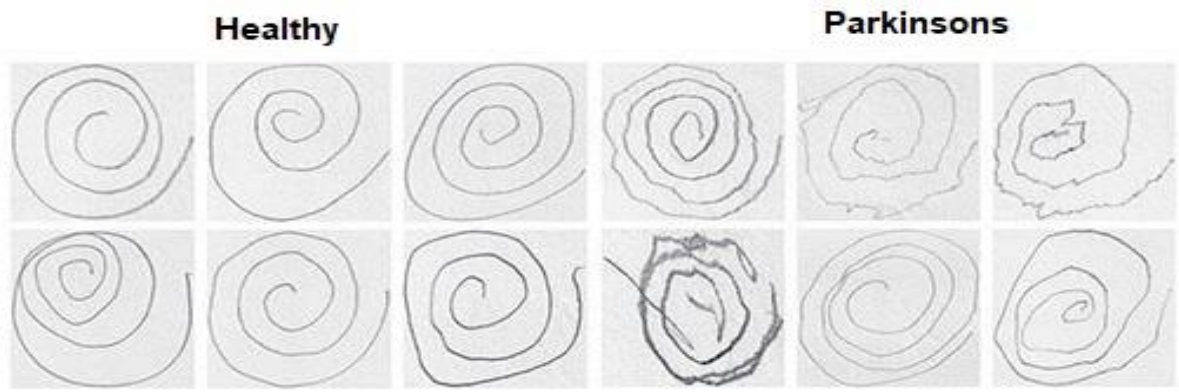

Figure 4. Samples of the spiral images.

A study by Zham et al. [63] revealed that individuals diagnosed with PD had reduced drawing speeds and decreased pen pressures, particularly among those with more severe forms of the condition. The visual characteristics of a hand-drawn spiral and wave may be directly impacted by the presence of tremors and muscle rigidity, which are two prominent manifestations of PD. This observation will be used in our analysis. The diversity in visual characteristics presents an opportunity to develop a computer vision and machine learning system capable of autonomously identifying PD. Figure 5 shows how patients draw a spiral.

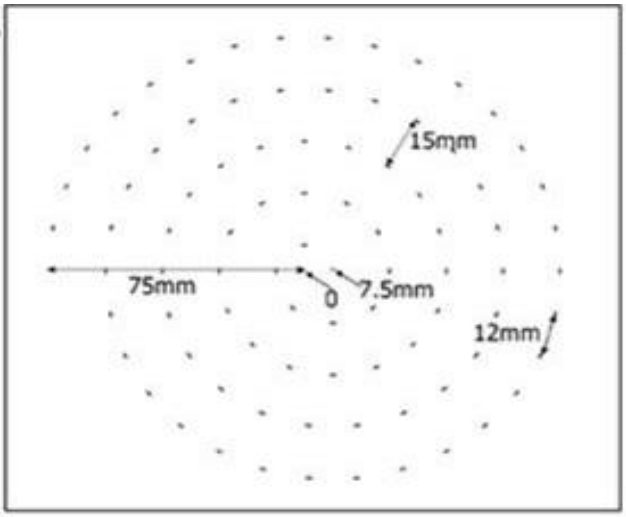

Figure 5. Patient to draw a spiral.

2.2. Preprocessing

The preprocessing method is a very important phase to enhance the DL models. The load_img function was used to load an image file. The function accepts the image file's path as its argument and outputs an object that represents the image. This process transformed the data into an array format. The function "img_to_array" was used to transform the imported image object into a NumPy array. During the process of converting the image into a NumPy array, a code proceeds the conversion to perform a division operation on the pixel values, dividing them by 244x244. Then, the pixel values are normalized to a range of 0 to 1. The process of normalizing the pixel values has been shown to enhance the convergence and performance of machine learning models.

2.3. Deep learning models

CNNs are deep learning models that can analyze and process visual images. CNNs are applied in a number of the real-life applications, such as brain-computer interfaces and time series analyses.

Transfer learning refers to the process of retaining and using problem-solving expertise in the context of other issue domains. Transfer learning leverages preexisting information to develop models that exhibit accelerated learning and need a reduced amount of training data. Transfer learning is a prominent area of study in the field of artificial intelligence, which involves the use of knowledge gained by addressing a particular problem and applying it to address a similar problem [64–66].

The CNN architecture consists of an activation function alongside convolution and pooling operations. The process of convolution involves taking an image and a filter as the input to produce an output image. The dimensions of the image, namely its size (244×244), height, breadth, and number of channels have a significant impact on the performance of the neural network.

$$C= \sum_1^i \sum_1^j I_{ij} F_{ij}. \tag{1}$$

The symbol F represents a convolution kernel or filter, whereas Ij represents rows and columns. The operation involves the multiplication of the image by the kernel, therefore presenting both the input image and the filter. The process of convolution involves decomposing the image into perceptrons, which are then flattened along the y-axis and z-axis. Each layer is equipped with a set of

x filters designed to detect and identify certain traits. Layer L produces feature maps of size X, which are then annotated as follows:

$$C_i^L = B_i^L + \sum_{j=1}^{x^{(L-1)}} F_{i,j}^L * C_j^{(L-1)}, \quad (2)$$

where B_i^L represents the bias matrix and $F_{i,j}^L$ denotes the value at position jth in the matrix F. The filter denoted as L serves as the connection between the jth feature map inside the layer. The CNN structure is presented in Figure 6.

2.3.1. DenseNet201 model

DenseNet is a CNN that uses dense blocks to directly link all layers with matching feature map sizes. Each layer receives inputs from previous layers and provides feature maps to succeeding levels to maintain the feed-forwardness. Every layer of the DenseNet undergoes a forward propagation process. These modifications result in a reduction of parameters, the mitigation of the vanishing-gradient problem, the enhancement of feature propagation, and the facilitation of reuse.

The DenseNet architecture has transition layers and dense blocks. Dense blocks consist of convolutional layers that are connected. A connection is established by connecting the output of each layer to the input of the subsequent layer. Transition layers are used in dense blocks to decrease the size of feature maps, which facilitates the development of the network. Figure 7 displays the architecture of the DenseNet model.

DenseNet201 is a CNN characterized by its increased depth, which effectively mitigates the issue of gradient disappearance, improves the propagation and use of features, and reduces the number of network parameters involved. The DenseNet201 model establishes direct connections between all levels to optimize information transfer. The proposed model demonstrates the construction of the dense block and transition layer submodules of DenseNet201. As with other models, DenseNet201 is trained using ImageNet.

DenseNet201 is transfer learning method that trains a model to identify and classify PD by using handwriting images. The DenseNet201 architecture consists of three dense blocks and four transition layers that connect these blocks. Each convolution layer inside the dense block is interconnected. The feature map undergoes expansion with each dense block. Transition layers are responsible for down sampling. The DenseNet201 architecture utilizes average pooling for down sampling. DenseNet201, which consists of 201 layers, is a variant. The object under consideration has substantial dimensions and possesses distinct layers of varying composition. The process of down sampling feature maps is accomplished using transition layers inside dense blocks. A pretrained model is generated using the same architectural frameworks. The model uses average pooling with the parameter pooling = “avg” to produce feature maps using pre-trained ImageNet weights. The pretrained model is a dense layer consisting of 256 units, which is activated using the rectified linear unit (ReLU) activation function. The proposed architecture of the modified DenseNet201 is shown in Figure 8. The parameters of the DenseNet201 model are presented in Table 2.

The image resizing process in the DenseNet 201 model involved adjusting the dataset images to a shape of (224x 224) to ensure compatibility with the input shape of the pre-trained DenseNet 201 model. Then, transfer learning was performed up to the 5×5 global average pooling layer located above the 256 fully connected (FC) layer. Subsequently, an FC layer was added, with the number of neurons corresponding to the classes used in the dataset. This FC layer was equipped with a soft max activation layer. The final layer’s weights were retrained using a learning rate of 0.001, the Adam optimizer, and

a batch size of 256 for a total of 50 epochs. Prior to using the DenseNet 201 model, it is essential to perform normalization preprocessing on the dataset images. Figure 9 illustrates the flow chart of the experimental method that used the DenseNet 201 model.

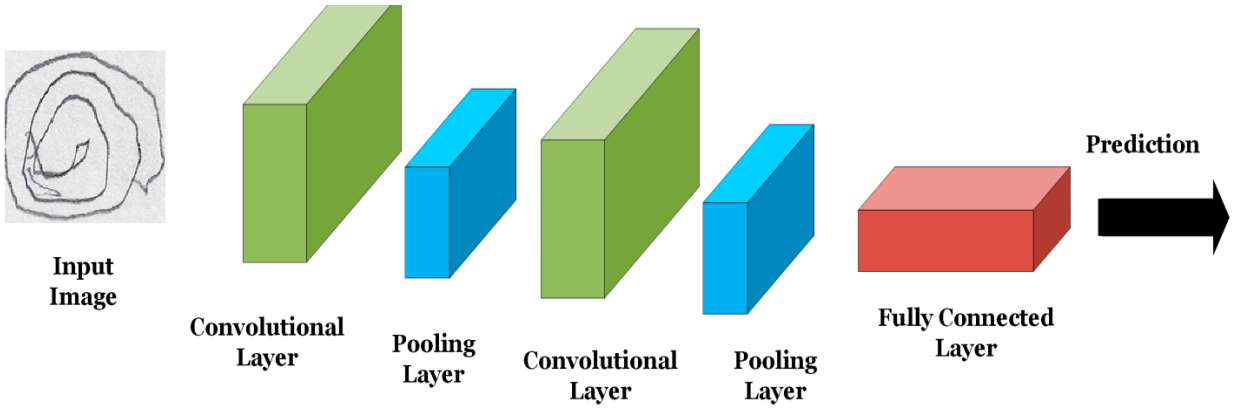

Figure 6. CNN model.

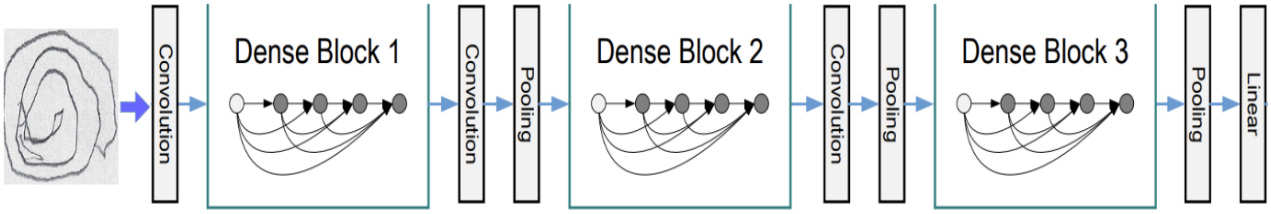

Figure 7. Structure of the DenseNet model.

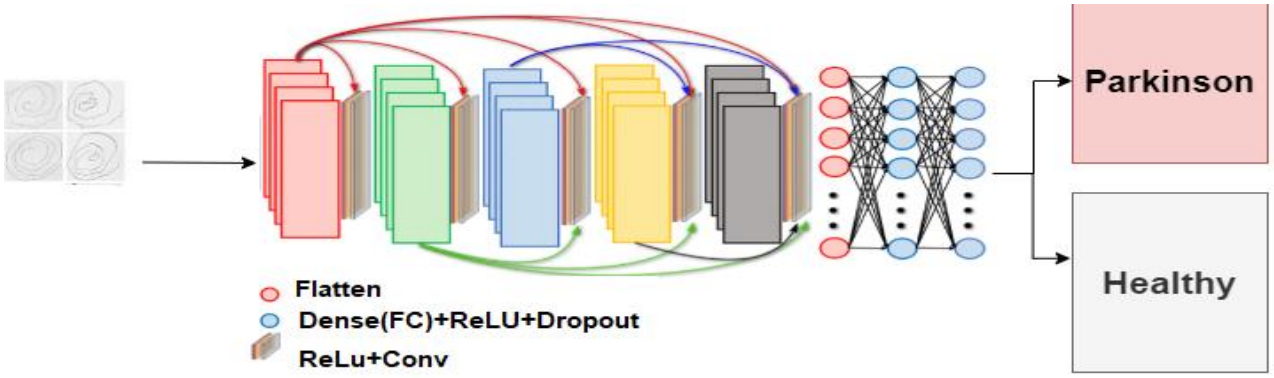

Figure 8. Architecture of modified DenseNet201.

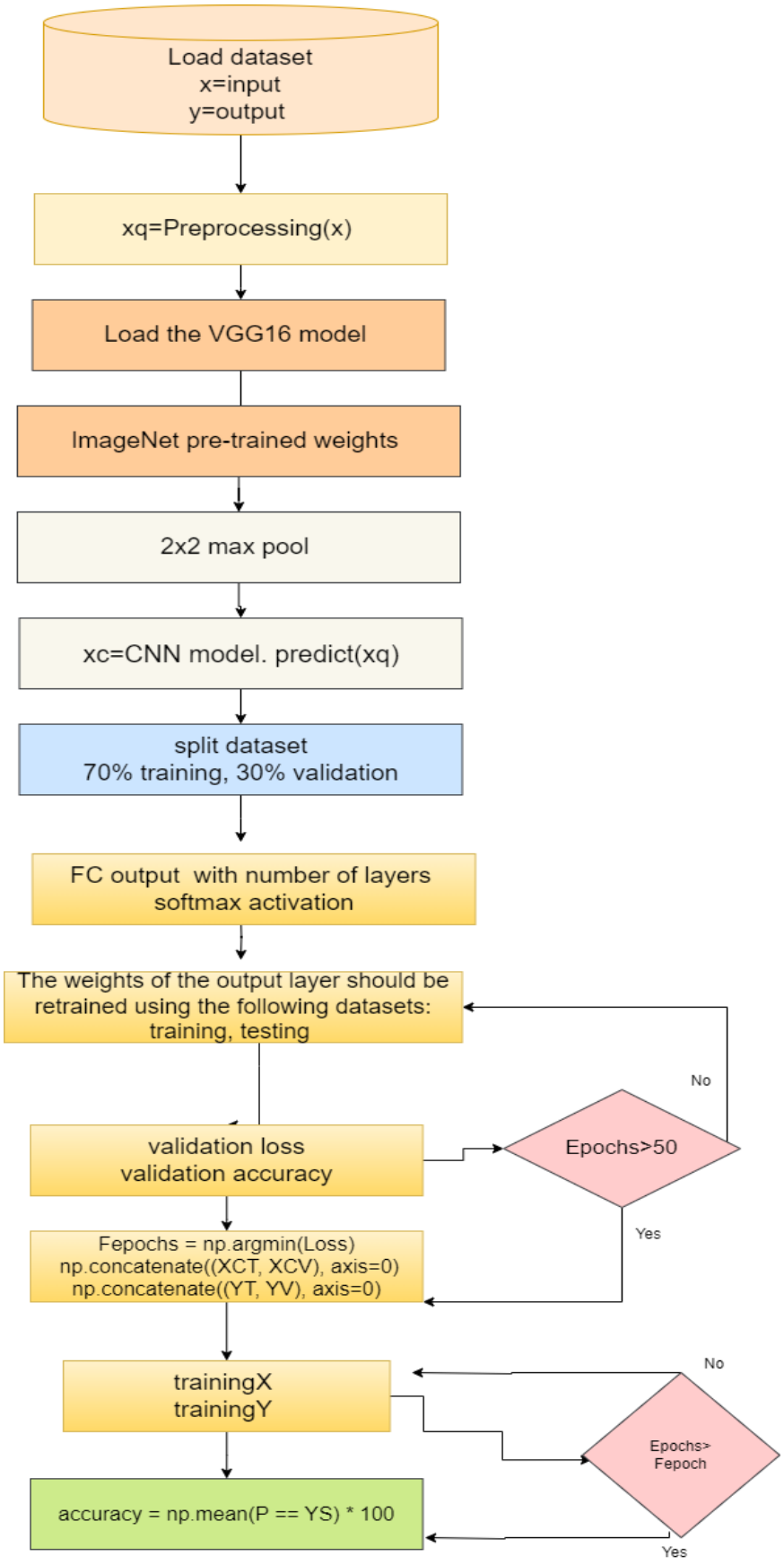

Figure 9. DenseNet201 flow chart.

Table 2. DenseNet201 parameters.

DenseNet 201 parameter setting	Details
Convolutional layer 1	256
Kernel size	5
Convolutional layer 2 number of filters	128
Kernel size	5
MaxPooling layer with pool size	5
Activation function	Softmax function using two outputs
Optimizer	Adam RMSprop
Number of epochs	60
Batch size	32

2.3.2. VGG16 model

VGGNet is a type of CNN that was collaboratively built by Google DeepMind and the Visual Geometry Group at the University of Oxford [57]. The VGG16 model is a CNN architecture consisting of 16 layers. The VGG16 model design prioritizes ConvNet layers with a kernel size of 3×3, as opposed to using several parameters. The minimum anticipated input image size for this model is 224x 224x 3 pixels, and it has three channels.

Optimization algorithms are often used in neural networks to assess the activation of individual neurons. This is achieved by calculating the weighted sum of the neuron's inputs. The use of a kernel function is motivated by the need to introduce nonlinearity into the output neuron. The neurons in a neural network are affected by weight, bias, and the associated training technique. The synaptic weights of the neurons are modified by the degree of discrepancy seen in the output. The inclusion of an input layer and the use of an activation function provide nonlinear characteristics that affect the input of artificial neural networks, and therefore enable them to acquire knowledge and successfully execute intricate tasks.

A pre-trained VGG16 model, specifically trained on the ImageNet dataset, is referred to in this study. The weights parameter is configured as "imagenet", thus suggesting the use of pre-trained weights. The process of immobilizing the layers in the base model is as follows. By assigning the value of "False" to the trainable attribute of each layer in the base_model, we effectively inhibit the modification of their weights throughout the training process. The global average pooling 2D function is a layer that applies global average pooling to decrease the spatial dimensions of feature maps. The dense layer, denoted as Dense (128, activation = "relu"), is a fully linked layer consisting of 256 units, which uses the rectified linear unit (ReLU) activation function. The output layer of the neural network is defined as Dense (two classes, activation = "softmax"). It consists of num_classes units and utilizes the softmax activation function to provide predicted class probabilities. The process of compiling the model is executed. The Adam optimizer was used with a learning rate of 0.0001. Figure 10 depicts the structure of the VGG16 model to detect PD. The VGG16 parameters are shown Table 3.

Table 3. VGG16 parameters.

VGG16 parameter settings	Values
Convolutional layer 1	256
Kernel size	5
Convolutional layer 2 number of filters	128
Kernel Size	5
MaxPooling layer with pool size	5
Activation function	Relu
Optimizer	Adam
Number of epochs	10
Batch size	32

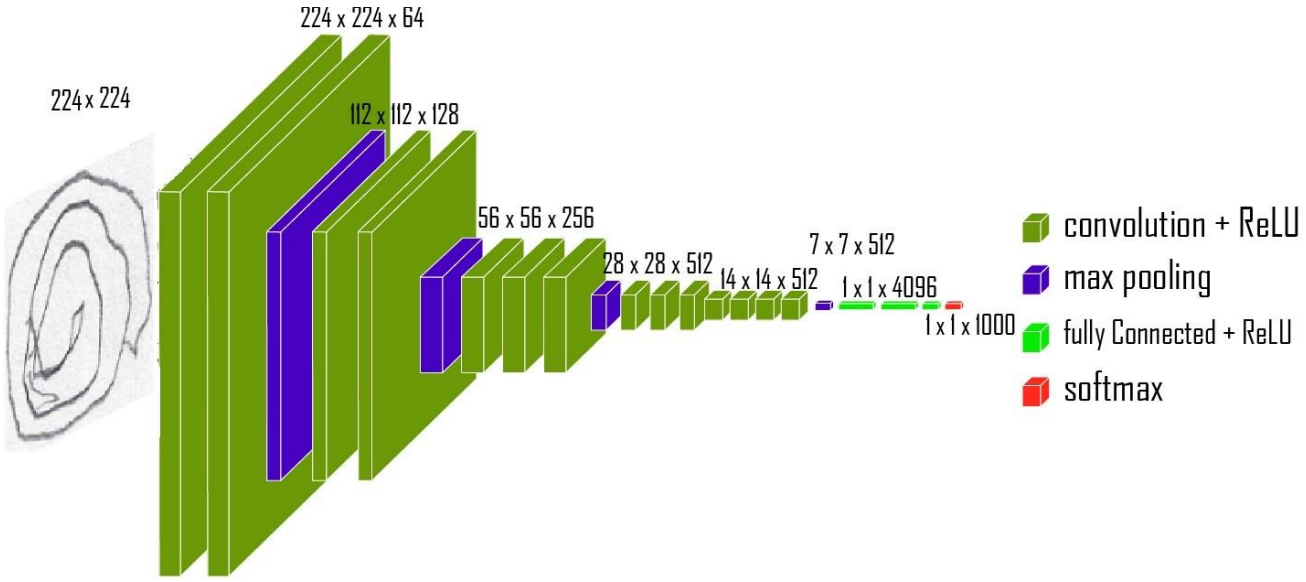

Figure 10. VGG16 framework.

The VGG 16 model involved resizing the images in the dataset to a shape of (224x 224x 3) in order to align with the input shape required by the pre-trained VGG 16 model. Then, transfer learning was performed up to the 5×5 max pooling layer in the block. The output of the pooling layer was flattened, followed by the addition of a ReLU activation layer. Then, a dropout regularization layer with a rate of 0.5 was added. Finally, a FC layer with a number of neurons equal to the number of classes in the dataset was added, along with a softmax activation layer. The final layer weights were retrained using a learning rate of 0.001, the Adam optimizer, and a batch size of 32 for a total of 50 epochs. Figure 11 depicts the flowchart illustrating the experimental methodology used, which utilized the VGG 16 model.

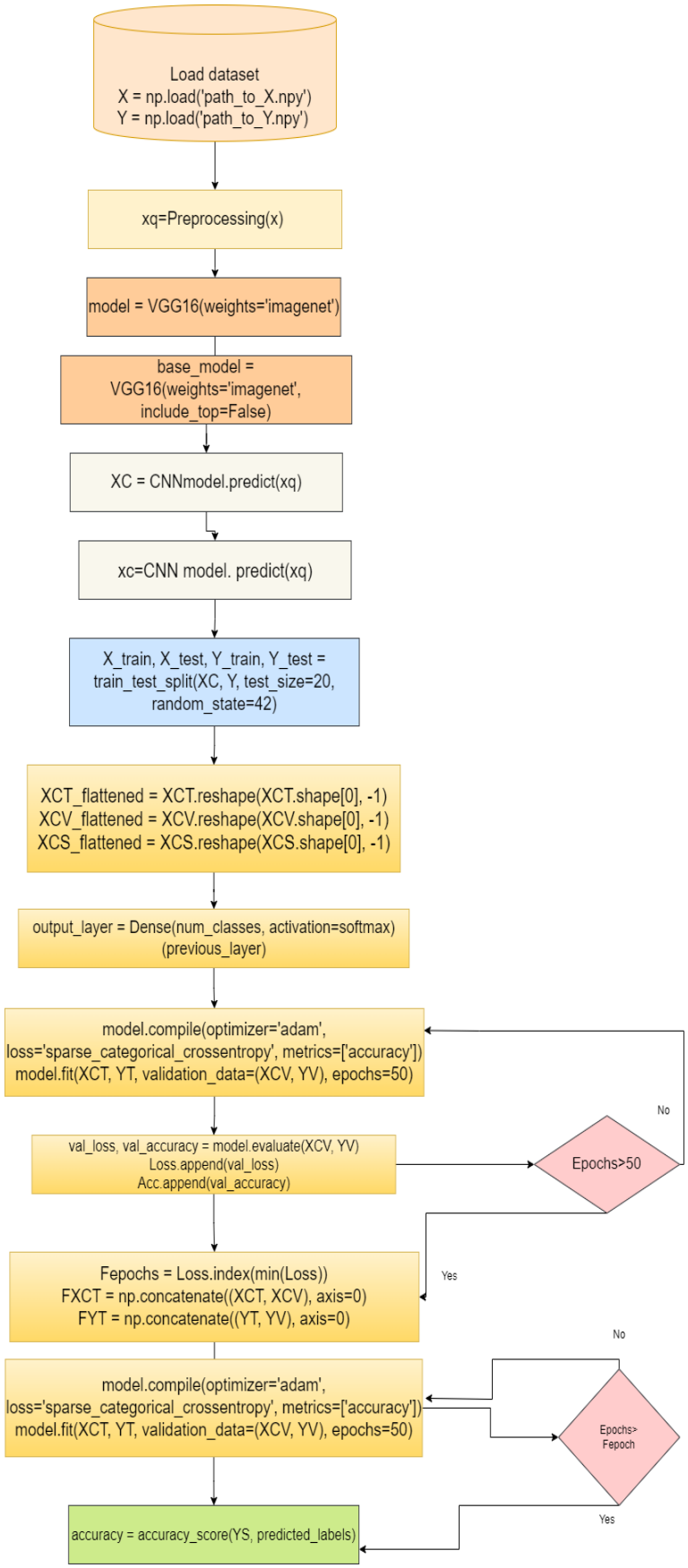

Figure 11. DenseNet201 flow chart.

3. Experiment

The investigation of medical decision support systems that provide precise biomarkers to clinicians for the detection of PD is a significant field of study. Nevertheless, the use of novel methodologies with DL models has the potential to provide clinicians with a non-invasive, uninterrupted, and unbiased approach to assist the monitoring of patients. Emerging technologies have the potential to assist healthcare professionals and authorities in identifying PD in its early stages.

This study used a handwriting analysis to determine if individuals diagnosed with PD had distinctive characteristics in their handwriting that could serve as tools for a PD diagnosis. A proposed system using DL has achieved a high level of accuracy in discriminating between those with normal cognitive function and those with PD.

3.1. Evaluation metrics

Evaluation metrics refer to quantitative measurements used to evaluate the performance of the DenseNet201 and VGG16 models. These metrics provide valuable insights into the performance of the model and facilitate the comparison of other models or algorithms.

$$Accuracy = \frac{TP+TN}{TP+FP+FN+TN} \times 100\%, \tag{3}$$

$$Sensitivity = \frac{TP}{TP+FN} \times 100\%, \tag{4}$$

$$Precision = \frac{TP}{TP+FP} \times 100\%, \tag{5}$$

$$specificity = \frac{TN}{TN+FP} \times 100\%, \tag{6}$$

$$F1 - score = 2 * \frac{precision \times Sensitivity}{precision + Sensitivity} \times 100\%. \tag{7}$$

3.2. Environmental setup

The hardware and software requirements play a crucial role in the functioning of this particular system. The suggested system aims to identify PD by analyzing the handwriting of both those without PD and those diagnosed with PD. Subsequently, the system is used to detect PD from images. In the experiments, a GPU system with 16 GB (RAM) and Windows OS was employed during the training and testing development the PD system. The system was developed by employing the Python 3.9 programming language. Several DL and ML libraries were used to develop the PD system, such as TensorFlow 13.2.0, Keras, and scikit-learn.

3.3. Data setting

The PD dataset was saved in a separate file, which was organized into two separate folders for training and testing. The total data was 204 images that consisted of spiral and wave patterns. The PD dataset was divided into a training set made up of 70% of the data and a testing set comprised of 30% of the data. Each directory of the dataset consisted of two subdirectories. One subdirectory included PD and healthy spiral images for the purposes of training and testing. The other subdirectory provided wave images of both PD and healthy individuals.

The ImageDataGenerator function provided a wide range of image augmentation techniques, such as rotation, shifting, shearing, zooming, flipping, and brightness adjustment. The implementation of these modifications augmented the diversity and uncertainty of the training dataset, thus resulting in enhancements in the efficacy and generalizability of the CNN model. This procedure involved the application of morphological transformations, such as rescaling, rotating within a range of 0 to 20 degrees, horizontal flipping, shifting the height within a range of 0 to 0.2, shearing within a range of 0 to 0.1, and zooming within a range of 0 to 0.2. Figure 12 shows the splitting of the spiral and wave datasets.

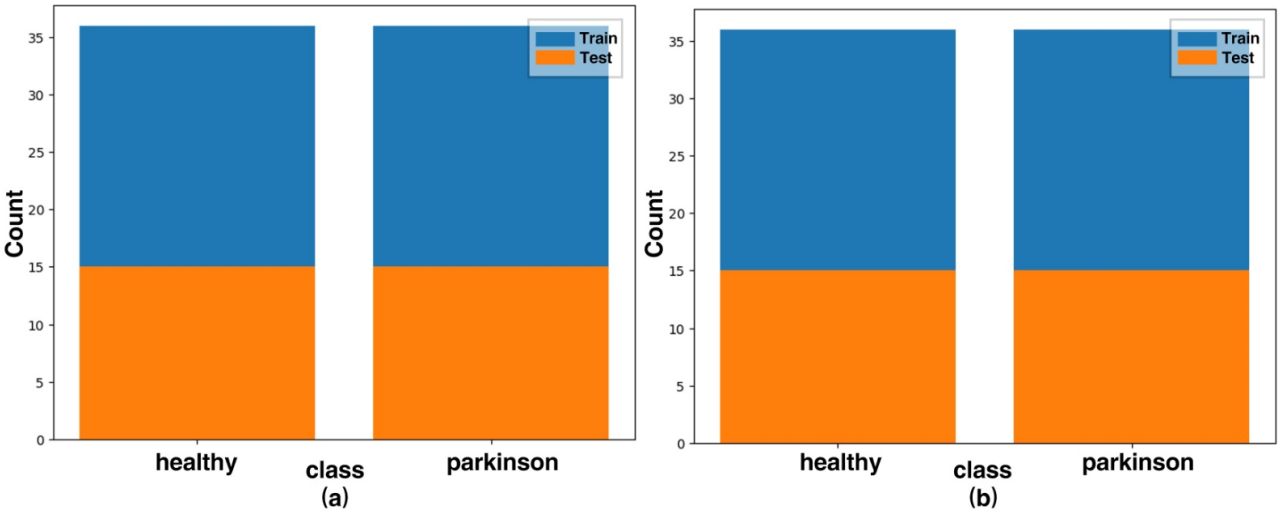

Figure 12. Classes a) spiral class b) wave class.

3.4. Deep learning results

This section presents the outcome results of the use of DL techniques to identify and classify PD while utilizing the spiral and wave drawings of PD patients.

3.4.1. Results of the DenseNet201 model

The DenseNet201 model was used to detect PD via the analysis of spiral and wave drawing images. The training procedure was conducted using a batch size of 32; each batch consisted of images with dimensions of 224×224. The training was carried out over a total of 60 epochs, and the early stopping technique was used based on the validation loss metric. Table 4 presents the outcomes obtained from the use of the DenseNet201 model to detect spiral images. Notably, the DenseNet201 model had a commendable accuracy rate of 94%. The DenseNet201 model achieved a high accuracy rate of 91% for identifying the normal class, as measured via a precision analysis. Additionally, it achieved a perfect recall and an F1-score of 95% for the same class.

Table 4. DenseNet201 model's ability to detect PD using spiral images.

	Precision %	Recall %	F1-score %	Accuracy %
Normal	91	100	95	94
Parkinson's	100	88	93	
Weighted avg	95	94	94	

The validation accuracy and loss were monitored throughout 60 epochs, and the training process was halted when the validation loss reached a value below the predetermined threshold of 0.5. At this point, the model achieved an accuracy of 94%, with a validation loss of 0.40. The accuracy of the DenseNet201 model is visualized in Figure 13, which depicts the convergence of the validation accuracy and loss and training loss over the training and validation processes, respectively.

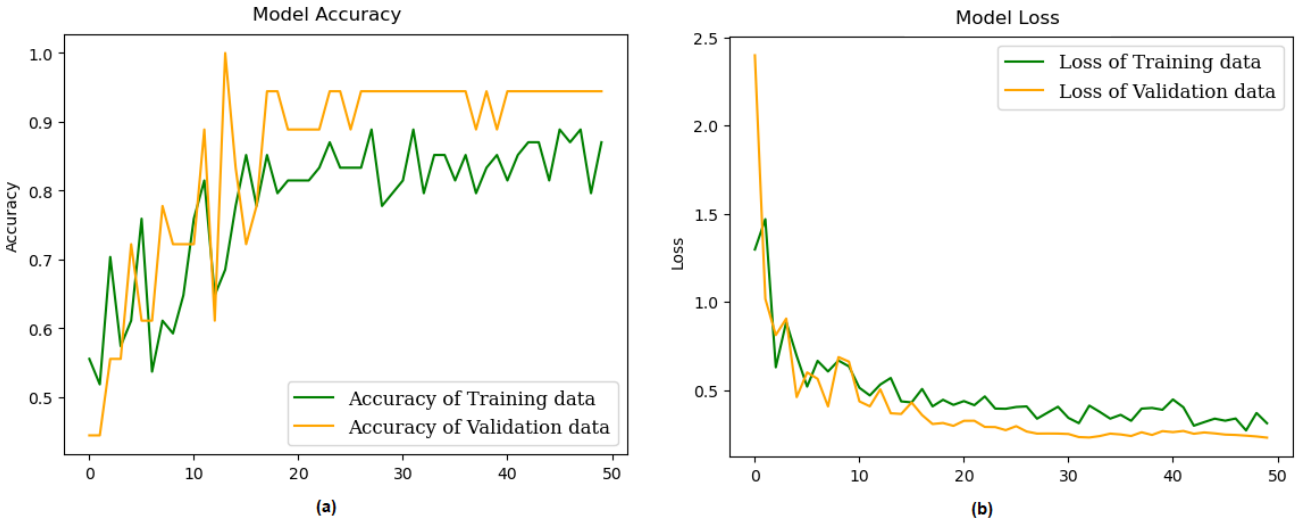

Figure 13. Performance of DenseNet201 model a) accuracy of DenseNet201 b) loss of DenseNet201.

The outcome results of the DenseNet201 model for identifying and classification PD using wave images is presented in Table5. The DenseNet201 model had a relatively lower accuracy rate of 89%. The DenseNet201 model has shown a lower accuracy in identifying PD using wave classification. The DenseNet201 model achieved weighted average scores of 91%, 89%, and 89% for their respective assessment measures.

Table 5. DenseNet201 model's ability to detect PD using wave images.

	Precision %	Recall %	F1-score %	Accuracy %
Normal	78	100	88	89
Parkinson's	100	82	90	
Weighted avg	91	89	89	

The model accuracy and loss of the DenseNet201 model for detecting the wave and spiral images for classifying PD is displayed in Figure 14. The validation accuracy exhibited fluctuations, with an initial value of 45% and a subsequent increase to over 89%. However, it stabilized at 55%, while the

training accuracy reached 80%. The model's accuracy loss begins at a value of 1.8 and gradually decreases to 0.4.

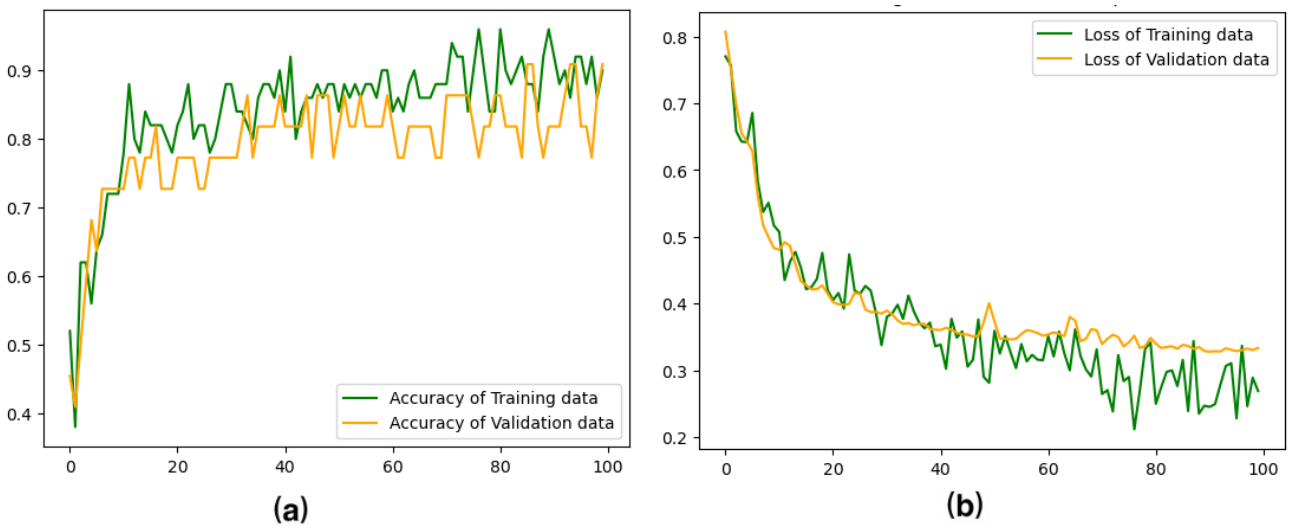

Figure 14. Performance of DenseNet201 model a) accuracy of DenseNet201 b) loss of DenseNet201.

3.4.2. Results of the VGG16 model

The VGG16 model was used to identify PD via the examination of spiral and wave images. The training approach was executed with a batch size of 32, whereby each batch was comprised of images with a demension of 240×240×3. The training procedure had a duration of 10 epochs, during which the early stopping strategy was used, relying on the validation loss measure. The results of the VGG16 model for detecting PD using spiral images are shown in Table 6. The VGG16 model achieved an accuracy rate of 80%. The VGG16 model achieved a weighted average precision of 82%, a recall of 80%, and an F1-score of 80%.

Table 6. The VGG16 model's ability to detect PD using spiral images.

	Precision %	Recall %	F1-score %	Accuracy %
Normal	74	93	82	80
Parkinson's	91	67	77	
Weighted avg	82	80	80	

Figure 15 presents the performance evaluation of the VGG16 model in identifying PD using spiral images. Starting from an initial accuracy 50% with 10 epochs, the training phase of VGG16 achieved an accuracy of 85%, while the testing procedure achieved an accuracy of 80%. The VGG16 loss begins with a value of 0.75 and then decreases to a final value of 0.42.

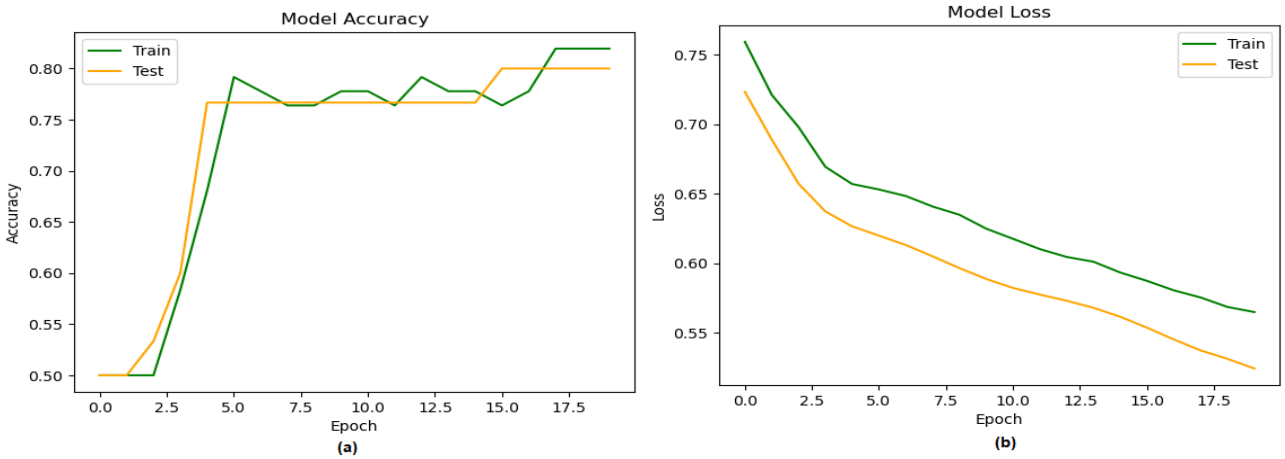

Figure 15. Performance of VGG16 model a) accuracy of VGG16 b) loss of VGG16.

The outcomes of the VGG16 model in terms of the detection of PD utilizing wave images are shown in Table 7. The VGG16 model achieved a high accuracy rate of 91% in the wave detection. The accuracy, recall, and F1-score parameters for evolution were weighted averaged at 92%, 91%, and 91%, respectively. In conclusion, it was found that the VGG16 model exhibited a superior performance in recognizing wave images as opposed to spiral images.

Table 7. The VGG16 model's ability to detect PD using wave images.

	Precision %	Recall %	F1-score %	Accuracy %
Normal	83	100	91	91
Parkinson's	100	83	91	
Weighted avg	92	91	91	

Figure 16 illustrates the efficacy of VGG16 in identifying PD by the use of wave images. At the beginning of the VGG16 model testing phase, the accuracy was 45%, which improved to 91%. The VGG16 model indicated comparable loss values throughout both the training and testing phases, starting at 0.75 and converging to 0.40.

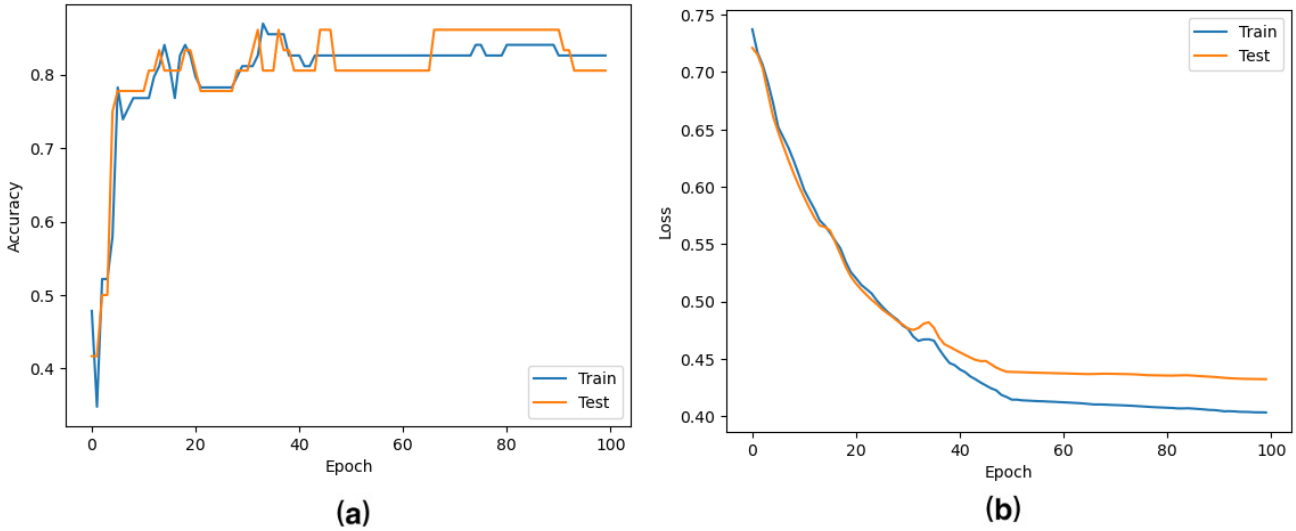

Figure 16. VGG16 performance model a) accuracy of VGG16 b) loss of VGG16.

4. Discussion and comparison

PD is a chronic and progressive condition that significantly impacts the quality of life of affected individuals. PPD remains incurable; hence, an early diagnosis offers the potential for an enhanced quality of life with appropriate medication, exercise, and therapeutic interventions. The first manifestation of this pathological condition is characterized by bradykinesia and tremors, which notably impact the motor skills involved in handwriting among affected individuals. There are several developed non-invasive methodologies for the diagnosis of PD by analyzing handwritten spirals produced by individuals affected by the condition.

PD is a neurodegenerative disorder characterized by the degeneration of cells within the nervous system. Initial indications include tremors or involuntary movements affecting the hands, arms, legs, and jaw. The artificial intelligence model has facilitated the development of applications that have the potential to assist in the diagnosis of PD without the need for clinical intervention. Handwriting irregularities are frequently identified in the majority of individuals afflicted with PD and are often described as one of the first manifestations of the condition. This study was conducted with a specific emphasis on the implications of handwriting on PD diagnosis.

In order to achieve the intended objective, a set of handwritten images was gathered from 204 people, including 102 individuals diagnosed with PD and 102 healthy individuals serving as the control. The dataset contained a collection of 204 spiral and wave images that served as training and testing data for a model designed to effectively categorize individuals with PD. Proposed transfer learning models, namely DenseNet201 and VGG16, were selected as the preferred approach DL models for detecting PD. In this study, many models of transfer learning were trained in order to determine the most suitable model. DenseNet201 had a 94% accuracy when detecting spiral images, whereas VGG16 achieved a high accuracy of 90% when detecting PD from wave images. This was found to be satisfactory, as shown by a testing accuracy of 94% and a testing accuracy of 90%.

The receiver operating characteristic (ROC) curve is a graphical representation that illustrates the classification model's performance across various categorization levels and represents the relationship between two variables. The ROC is calculated as follows:

$$TRP=\frac{TP}{TP+FN} \tag{5}$$

$$FPR=\frac{FP}{FP+TN} \tag{6}$$

where TRP is the true positive rate and FPR is the false positive rate.

The ROC curve of the DenseNet201 model is shown in Figure 17. The ROC metric is calculated based on the false positive rate (FPR) of the DenseNet201 model. When utilizing spiral images, the FPR is 1, whereas when using wave images, the FPR is 2. Therefore, the performance of the DenseNet201 model achieved a classification accuracy of 99% when trained on spiral images; however, it achieved a classification accuracy of only 95% when trained on wave images. The DenseNet201 model notably achieved a high accuracy when trained on spiral images.

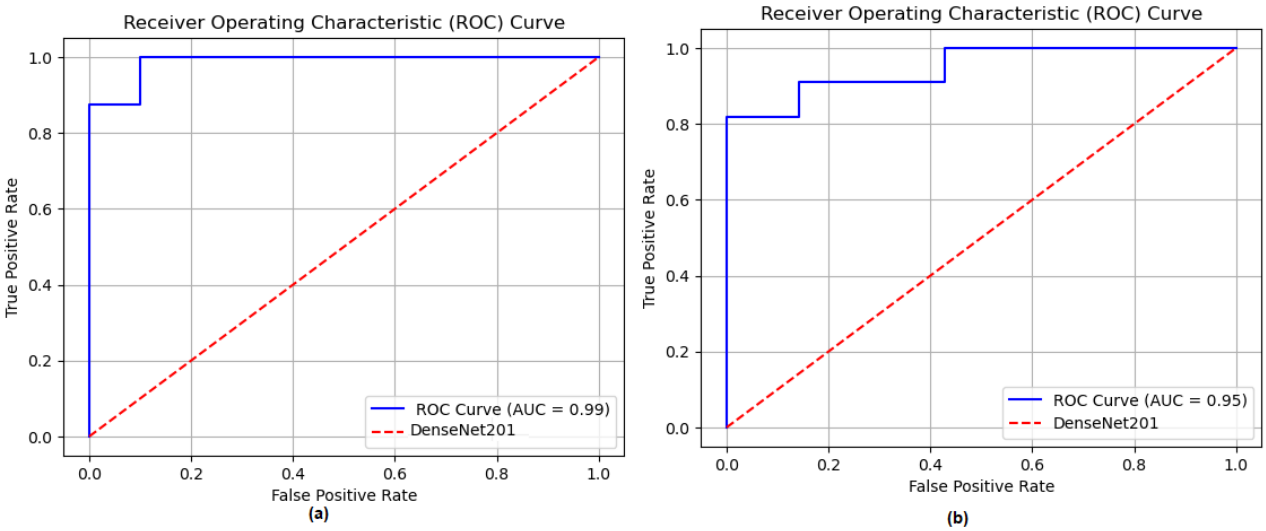

Figure 17. ROC of DenseNet201 model.

Figure 18 presents the ROC curve of the VGG16 model in the context of identifying PD using spiral and wave images. The VGG16 model achieved a high accuracy rate by using wave images. The use of spiral images resulted in a reduced percentage of 90% or less for the ROC. The ROC was observed to be 80%.

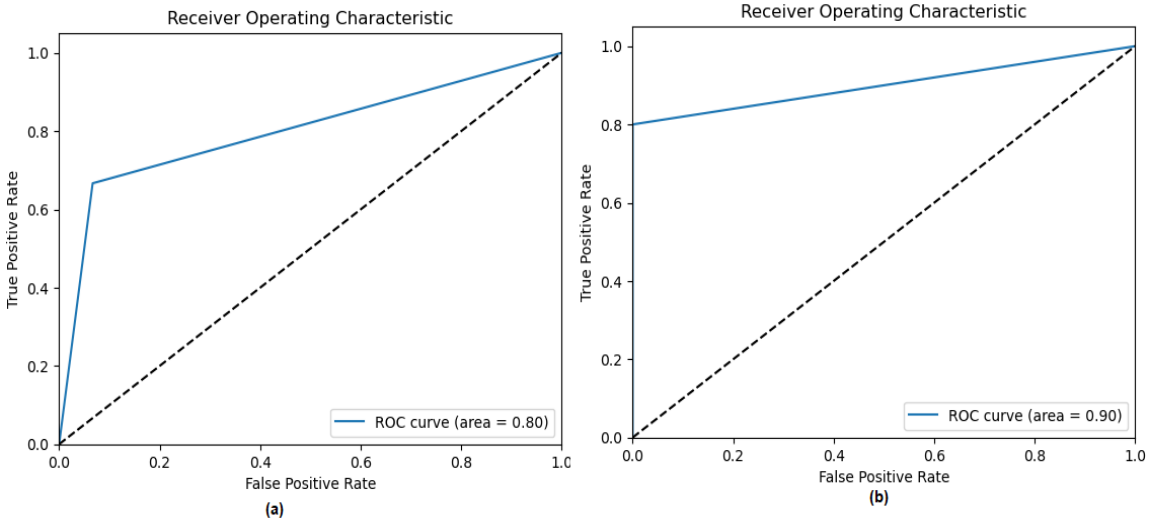

Figure 18. ROC of VGG16 model.

We assessed the efficacy of our proposed model, which demonstrated a validation accuracy of the DenseNet201 and VGG16 models, as compared with various existing systems. Authors [41] used RF, CNN, and Resnet50 to detect PD using spiral and wave drawing images. The author used a similar dataset, where it was observed that the CNN and ResNet50 achieved 90%. The CNN used spiral images, while RestNet50 achieved 87% accuracy using wave images. Authors in [42] used the lightning CNN model and achieved an accuracy of 63.33%. Researchers in [52] used a CNN to identify PD based on spiral and wave images. The results indicated that the CNN model achieved an accuracy of 88% when recognizing PD from spiral images, and 89% when detecting PD from wave images. Approximately 80% of the models underwent training and validation processes. The SqueezeNet model obtained an

accuracy of 72.53%, whereas AlexNet achieved an accuracy of 76.76% and MobileNet achieved an accuracy of 76.56%. The results are shown in Table 8. Figure 19 displays a graphical representation that compares the suggested systems using DL with the current systems.

Table 8. Results of DenseNet201 and VGG16 models against the existing PD systems.

Ref.	Models	Dataset	Accuracy	ROC
Ref. [59]	RF CNN ResNet50	Same dataset 204 spiral and wave images	Wave images=80% Spiral image=67% Wave images=87% Spiral image=90% Wave images=87% Spiral image=90%	
Ref. [60]	Lightning CNN	Same dataset used Spiral images	Spiral image=63.33%	
Ref. [61]	CNN	Same dataset 204 spiral and wave images	Wave images=88% Spiral image=89%	
Ref. [62]	CNN	Same dataset 204 spiral and wave images	Wave images=73% Spiral image=83%	
Our enhanced models	DenseNet201 VGG16	Same dataset 204 spiral and wave images	Spiral images=94% Wave image=91%	99% 90%

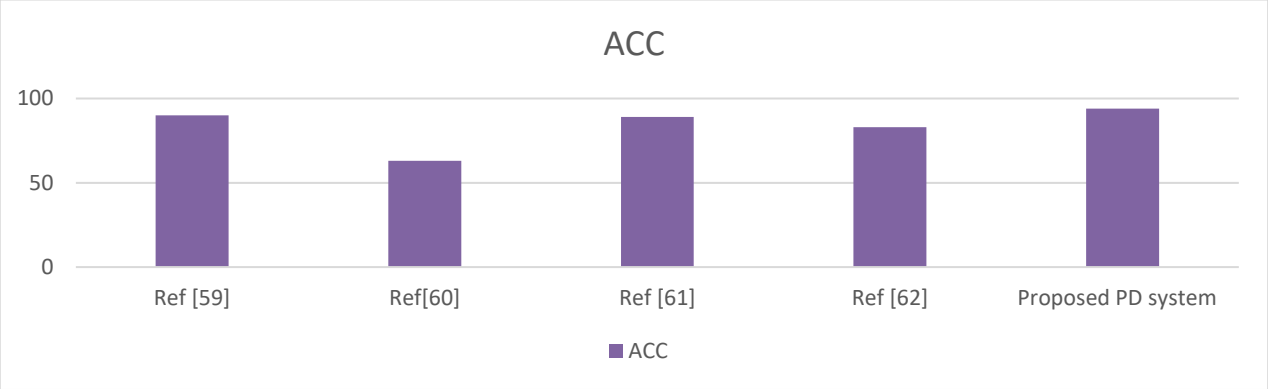

Figure 19. Performance of the PD system by evaluating with existing PD systems.

5. Conclusions

Identification of PD poses significant challenges and necessitates the use of biomarkers in conjunction with symptomatic manifestations, such as tremors, bradykinesia, and stiffness, to enhance diagnostic precision.

The identification of PD would enable the formulation and implementation of targeted therapeutic approaches for those affected by this condition. PD completely affects the routine schedule life of patients. Detecting PD at its earliest stages helps physicians to treat patients better. To improve the detection of PD, DL models were presented in this research. This study showed that observations of spiral and wave drawings can help physicians distinguish between patients with PD and healthy

patients. The proposed system used a standard dataset containing 204 spiral and wave drawings from Parkinson's patients. DL models such as DenseNet201 and VGG16 were applied to detect PD.

The objective of this study was to enhance the diagnostic process of PD using DL models. The primary goal was to discern between those without PD (healthy) and those diagnosed with PD. The emphasis of our methodology was the identification of anomalies in the locomotion patterns of patients via the use of drawing images. Furthermore, this study investigates the relative effectiveness of two drawing tasks, namely spiral and wave, in the discriminating process. The DenseNet201 classifier, which was trained using images of the spiral drawing task, was 94% accurate and had a ROC score of 99%. This suggests that it may serve as an effective and unbiased tool to distinguish individuals with PD from healthy individuals. The VGG16 model was used to discern between individuals with PD and healthy controls using wave images, achieving a notable accuracy rate of 91% and a ROC score of 90%. The use of DL techniques may be explored in future research to enhance the performance of the DenseNet201 and VGG16 models.

Use of AI tools declaration

The authors declare they have not used Artificial Intelligence (AI) tools in the creation of this article.

Acknowledgments

The authors extend their appreciation to the king Salman center for disability research for funding this work through research group No: KSGR-2023-236.

Conflict of interest

The authors declare no conflicts of interest.

Data availability statement

Available from: https://www.kaggle.com/datasets/kmader/parkinsons-drawings/data (accessed on 2 August 2023).

References

1. C. G. Goetz, The history of Parkinson's disease: early clinical descriptions and neurological therapies, *Cold Spring Harb. Perspect. Med.*, **1** (2011), a008862. https://doi.org/10.1101/cshperspect.a008862
2. S. D. Vassar, Y. M. Bordelon, R. D. Hays, N. Diaz, R. Rausch, C. Mao, et al., Confirmatory factor analysis of the motor unified Parkinson's disease rating scale, *Park. Dis.*, **2012** (2012), 719167. https://doi.org/10.1155/2012/719167
3. *Parkinson disease*, World Health Organization, 9 August 2023. Available online: https://www.who.int/news-room/fact-sheets/detail/parkinson-disease.

4. M. C. De Rijk, L. J. Launer, K. Berger, M. M. Breteler, J. F. Dartigues, M. Baldereschi, et al., Prevalence of Parkinson's disease in Europe: a collaborative study of population-based cohorts: neurologic diseases in the elderly research group, *Neurology*, **54** (2000), S21–S23.
5. İ. Cantürk, F. Karabiber, A machine learning system for the diagnosis of Parkinson's disease from speech signals and its application to multiple speech signal types, *Arab. J. Sci. Eng.*, **41** (2016), 5049–5059. https://doi.org/10.1007/s13369-016-2206-3
6. N. Singh, V. Pillay, Y. E. Choonara, Advances in the treatment of Parkinson's disease, *Prog. Neurobiol.*, **81** (2007), 29–44. https://doi.org/10.1016/j.pneurobio.2006.11.009
7. A. Rana, A. S. Rawat, A. Bijalwan, H. Bahuguna, Application of multi-layer (perceptron) artificial neural network in the diagnosis system: a systematic review, *2018 International Conference on Research in Intelligent and Computing in Engineering (RICE)*, IEEE, 2018, 1–6. https://doi.org/10.1109/RICE.2018.8509069
8. L. F. Gomez-Gomez, A. Morales, J. Fierrez, J. R. Orozco-Arroyave, Exploring facial expressions and affective domains for Parkinson detection, *arXiv*, 2020. https://doi.org/10.48550/arXiv.2012.06563
9. A. M. García, T. Arias-Vergara, J. C. Vasquez-Correa, E. Nöth, M. Schuster, A. E. Welch, et al., Cognitive determinants of dysarthria in Parkinson's disease: an automated machine learning approach, *Mov. Disord.*, **36** (2021), 2862–2873. https://doi.org/10.1002/mds.28751
10. A. Birba, I. García-Cordero, G. Kozono, A. Legaz, A. Ibáñez, L. Sedeño, et al., Losing ground: frontostriatal atrophy disrupts language embodiment in Parkinson's and Huntington's disease, *Neurosci. Biobehav. Rev.*, **80** (2017), 673–687. https://doi.org/10.1016/j.neubiorev.2017.07.011
11. J. Dolz, C. Desrosiers, I. B. Ayed, 3D fully convolutional networks for subcortical segmentation in MRI: a large-scale study, *NeuroImage*, **170** (2018), 456–470. https://doi.org/10.1016/j.neuroimage.2017.04.039
12. M. Ghafoorian, N. Karssemeijer, T. Heskes, I. W. van Uden, C. I. Sanchez, G. Litjens, et al., Location sensitive deep convolutional neural networks for segmentation of white matter hyperintensities, *Sci. Rep.*, **7** (2017), 5110. https://doi.org/10.1038/s41598-017-05300-5
13. S. H. Wang, P. Phillips, Y. Sui, B. Liu, M. Yang, H. Cheng, Classification of Alzheimer's disease based on eight-layer convolutional neural network with leaky rectified linear unit and max pooling, *J. Med. Syst.*, **42** (2018), 85. https://doi.org/10.1007/s10916-018-0932-7
14. M. Younis Thanoun, M. T. Yaseen, A comparative study of Parkinson disease diagnosis in machine learning, *Proceedings of the 2020 the 4th International Conference on Advances in Artificial Intelligence*, 2020, 23–28. https://doi.org/10.1145/3441417.3441425
15. T. Elhassan, M. Aljurf, Classification of imbalance data using Tomek link (T-link) combined with random under-sampling (RUS) as a data reduction method, *Glob. J. Technol. Optim.*, **1** (2016), 1–11. https://doi.org/10.4172/2229-8711.S1:111
16. S. Fan, Y. Sun, Early detection of Parkinson's disease using machine learning and convolutional neural networks from drawing movements, *CS & IT Conference Proceedings*, **12** (2022), 291–301. https://doi.org/10.5121/csit.2022.121523
17. P. Arora, A. Mishra, A. Malhi, Machine learning Ensemble for the Parkinson's disease using protein sequences, *Multimed. Tools Appl.*, **81** (2022), 32215–32242. https://doi.org/10.1007/s11042-022-12960-7
18. Shivangi, A. Johri, A. Tripathi, Parkinson disease detection using deep neural networks, *2019 Twelfth International Conference on Contemporary Computing (IC3)*, 2019, 1–4. https://doi.org/10.1109/IC3.2019.8844941

19. D. A. Rastegar, N. Ho, G. M. Halliday, N. Dzamko, Parkinson's progression prediction using machine learning and serum cytokines, *npj Parkinsons. Dis.*, **5** (2019), 14. https://doi.org/10.1038/s41531-019-0086-4
20. M. Nilashi, H. Ahmadi, A. Sheikhtaheri, R. Naemi, R. Alotaibi, A. A. Alarood, et al., Remote tracking of Parkinson's disease progression using ensembles of deep belief network and self-organizing map, *Expert Syst. Appl.*, **159** (2020), 113562. https://doi.org/10.1016/j.eswa.2020.113562
21. R. Das, A comparison of multiple classification methods for diagnosis of Parkinson disease, *Expert Syst. Appl.*, **37** (2010), 1568–1572. https://doi.org/10.1016/j.eswa.2009.06.040
22. Saloni, R. K. Sharma, A. K. Gupta, Voice analysis for telediagnosis of Parkinson disease using artificial neural networks and support vector machines, *Int. J. Intell. Syst. Appl.*, **7** (2015), 41–47. https://doi.org/10.5815/ijisa.2015.06.04
23. H. L. Chen, G. Wang, C. Ma, Z. N. Cai, W. B. Liu, S. J. Wang, An efficient hybrid kernel extreme learning machine approach for early diagnosis of Parkinson's disease, *Neurocomputing*, **184** (2016), 131–144. https://doi.org/10.1016/j.neucom.2015.07.138
24. N. M. Tahir, Parkinson disease gait classification based on machine learning approach, *J. Appl. Sci.*, **12** (2012), 180–185. https://doi.org/10.3923/jas.2012.180.185
25. E. Abdulhay, N. Arunkumar, K. Narasimhan, E. Vellaiappan, V. Venkatraman, Gait and tremor investigation using machine learning techniques for the diagnosis of Parkinson disease, *Futur. Gener. Comput. Syst.*, **83** (2018), 366–373. https://doi.org/10.1016/j.future.2018.02.009
26. Y. N. Zhang, Can a smartphone diagnose Parkinson disease? A deep neural network method and telediagnosis system implementation, *Park. Dis.*, **2017** (2017), 6209703. https://doi.org/10.1155/2017/6209703
27. G. Nagasubramanian, M. Sankayya, Multi-Variate vocal data analysis for detection of Parkinson disease using deep learning, *Neural Comput. Appl.*, **33** (2020), 4849–4864. https://doi.org/10.1007/s00521-020-05233-7
28. I. El Maachi, G. A. Bilodeau, W. Bouachir, Deep 1D-convnet for accurate Parkinson disease detection and severity prediction from gait, *Expert Syst. Appl.*, **143** (2020), 113075. https://doi.org/10.1016/j.eswa.2019.113075
29. A. Naseer, M. Rani, S. Naz, M. I. Razzak, M. Imran, G. Xu, Refining Parkinson's neurological disorder identification through deep transfer learning, *Neural Comput. Appl.*, **32** (2020), 839–854. https://doi.org/10.1007/s00521-019-04069-0
30. S. Shinde, S. Prasad, Y. Saboo, R. Kaushick, J. Saini, P. K. Pal, et al., Predictive markers for Parkinson's disease using deep neural nets on neuromelanin sensitive MRI, *NeuroImage Clin.*, **22** (2019), 101748. https://doi.org/10.1016/j.nicl.2019.101748
31. S. L. Oh, Y. Hagiwara, U. Raghavendra, R. Yuvaraj, N. Arunkumar, M. Murugappan, et al., A deep learning approach for Parkinson's disease diagnosis from EEG signals, *Neural Comput. Appl.*, **32** (2020), 10927–10933. https://doi.org/10.1007/s00521-018-3689-5
32. J. C. Vasquez-Correa, T. Arias-Vergara, J. R. Orozco-Arroyave, B. M. Eskofier, J. Klucken, E. Noth, Multimodal assessment of Parkinson's disease: a deep learning approach, *IEEE J. Biomed. Health Inform.*, **23** (2019), 1618–1630. https://doi.org/10.1109/JBHI.2018.2866873
33. A. Talitckii, E. Kovalenko, A. Anikina, O. Zimniakova, M. Semenov, E. Bril, et al., Avoiding misdiagnosis of Parkinson's disease with the use of wearable sensors and artificial intelligence, *IEEE Sensors J.*, **21** (2021), 3738–3747. https://doi.org/10.1109/JSEN.2020.3027564

34. C. R. Pereira, D. R. Pereira, F. A. da Silva, C. Hook, S. A. Weber, L. A. M. Pereira, et al., A step towards the automated diagnosis of Parkinson's disease: analyzing handwriting movements, *2015 IEEE 28th International Symposium on Computer-Based Medical Systems*, 2015, 171–176. https://doi.org/10.1109/CBMS.2015.34
35. C. R. Pereira, D. R. Pereira, J. P. Papa, G. H. Rosa, X. S. Yang, Convolutional neural networks applied for Parkinson's disease identification, In: A. Holzinger, *Machine learning for health informatics. lecture notes in computer science*, Cham: Springer, **9605** (2016), 377–390. https://doi.org/10.1007/978-3-319-50478-0_19
36. C. R. Pereira, D. R. Pereira, G. H. Rosa, V. H. Albuquerque, S. A. Weber, C. Hook, et al., Handwritten dynamics assessment through convolutional neural networks: an application to Parkinson's disease identification, *Artif. Intell. Med.*, **87** (2018), 67–77. https://doi.org/10.1016/j.artmed.2018.04.001
37. M. Shaban, Deep convolutional neural network for Parkinson's disease based handwriting screening, *2020 IEEE 17th International Symposium on Biomedical Imaging Workshops (ISBI Workshops)*, 2020, 1–4. https://doi.org/10.1109/ISBIWorkshops50223.2020.9153407
38. T. J. Wroge, Y. Ozkanca, C. Demiroglu, D. Si, D. C. Atkins, R. H. Ghomi, Parkinson's disease diagnosis using machine learning and voice, *2018 IEEE Signal Processing in Medicine and Biology Symposium (SPMB)*, 2018, 1–7. https://doi.org/10.1109/SPMB.2018.8615607
39. Y. Dai, Z. Tang, Y. Wang, Z. Xu, Data driven intelligent diagnostics for Parkinson's disease, *IEEE Access*, **7** (2019), 106941–106950. https://doi.org/10.1109/ACCESS.2019.2931744
40. J. Rusz, M. Novotny, J. Hlavnicka, T. Tykalova, E. Ruzicka, High-accuracy voice-based classification between patients with Parkinson's disease and other neurological diseases may be an easy task with inappropriate experimental design, *IEEE Trans. Neural Syst. Rehabil. Eng.*, **25** (2017), 1319–1321. https://doi.org/10.1109/TNSRE.2016.2621885
41. A. U. Haq, J. P. Li, M. H. Memon, J. Khan, A. Malik, T. Ahmad, et al., Feature selection based on L1-norm support vector machine and effective recognition system for Parkinson's disease using voice recordings, *IEEE Access*, **7** (2019), 37718–37734. https://doi.org/10.1109/ACCESS.2019.2906350
42. J. Prince, F. Andreotti, M. De Vos, Multi-source ensemble learning for the remote prediction of Parkinson's disease in the presence of source-wise missing data, *IEEE Trans. Biomed. Eng.*, **66** (2019), 1402–1411. https://doi.org/10.1109/TBME.2018.2873252
43. W. Zeng, F. Liu, Q. Wang, Y. Wang, L. Ma, Y. Zhang, Parkinson's disease classification using gait analysis via deterministic learning, *Neurosci. Lett.*, **633** (2016), 268–278. https://doi.org/10.1016/j.neulet.2016.09.043
44. A. Muniz, H. Liu, K. Lyons, R. Pahwa, W. Liu, F. Nobre, et al., Comparison among probabilistic neural network, support vector machine and logistic regression for evaluating the effect of subthalamic stimulation in Parkinson disease on ground reaction force during gait, *J. Biomech.*, **43** (2010), 720–726. https://doi.org/10.1016/j.jbiomech.2009.10.018
45. F. M. J. Pfister, T. T. Um, D. C. Pichler, J. Goschenhofer, K. Abedinpour, M. Lang, et al., High-resolution motor state detection in Parkinson's disease using convolutional neural networks, *Sci. Rep.*, **100** (2020), 5860. https://doi.org/10.1038/s41598-020-61789-3
46. P. Drotár, J. Mekyska, I. Rektorová, L. Masarová, Z. Smékal, M. Faundez-Zanuy, Analysis of in-air movement in handwriting: a novel marker for Parkinson's disease, *Comput. Methods Programs Biomed.*, **117** (2014), 405–411. https://doi.org/10.1016/j.cmpb.2014.08.007

47. M. I. Vanegas, M. F. Ghilardi, S. P. Kelly, A. Blangero, Machine learning for EEG-based biomarkers in Parkinson's disease, *2018 IEEE International Conference on Bioinformatics and Biomedicine (BIBM)*, 2018, 2661–2665. https://doi.org/10.1109/BIBM.2018.8621498
48. S. L. Oh, Y. Hagiwara, U. Raghavendra, R. Yuvaraj, N. Arunkumar, M. Murugappan, et al., A deep learning approach for Parkinson's disease diagnosis from EEG signals, *Neural Comput. Appl.*, **32** (2018), 10927–10933. https://doi.org/10.1007/s00521-018-3689-5
49. N. Wagh, Y. Varatharajah, EEG-GCNN: augmenting electroencephalogram-based neurological disease diagnosis using a domain-guided graph convolutional neural network, *Proc. Mach. Learn. Res.*, **136** (2020), 367–378.
50. X. Shi, T. Wang, L. Wang, H. Liu, N. Yan, Hybrid convolutional recurrent neural networks outperform CNN and RNN in task-state EEG detection for Parkinson's disease, *2019 Asia-Pacific Signal and Information Processing Association Annual Summit and Conference (APSIPA ASC)*, 2019, 18–21. https://doi.org/10.1109/APSIPAASC47483.2019.9023190
51. X. Zhang, Y. Yang, H. Wang, S. Ning, H. Wang, Deep neural networks with broad views for Parkinson's disease screening, *2019 IEEE International Conference on Bioinformatics and Biomedicine (BIBM)*, 2019, 1018–1022. https://doi.org/10.1109/BIBM47256.2019.8983000
52. V. M. Ramirez, V. Kmetzsch, F. Forbes, M. Dojat, Deep learning models to study the early stages of Parkinson's disease, *2020 IEEE 17th International Symposium on Biomedical Imaging (ISBI)*, 2020, 1534–1537. https://doi.org/10.1109/ISBI45749.2020.9098529
53. J. Prasuhn, M. Heldmann, T. F. Münte, N. Brüggemann, A machine learning-based classification approach on Parkinson's disease diffusion tensor imaging datasets, *Neurol. Res. Pract.*, **2** (2020), 46. https://doi.org/10.1186/s42466-020-00092-y
54. J. Rasheed, A. A. Hameed, N. Ajlouni, A. Jamil, A. Ozyavas, Z. Orman, Application of adaptive back-propagation neural networks for Parkinson's disease prediction, *2020 International Conference on Data Analytics for Business and Industry: Way Towards a Sustainable Economy (ICDABI)*, 2020, 1–5. https://doi.org/10.1109/ICDABI51230.2020.9325709
55. H. Gunduz, Deep learning-based Parkinson's disease classification using vocal feature sets, *IEEE Access*, **7** (2019), 115540–115551. https://doi.org/10.1109/ACCESS.2019.2936564
56. S. Moon, H. J. Song, V. D. Sharma, K. E. Lyons, R. Pahwa, A. E. Akinwuntan, et al., Classification of Parkinson's disease and essential tremor based on balance and gait characteristics from wearable motion sensors via machine learning techniques: a data-driven approach, *J. NeuroEng. Rehabil.*, **17** (2020), 125. https://doi.org/10.1186/s12984-020-00756-5
57. W. Zeng, F. Liu, Q. Wang, Y. Wang, L. Ma, Y. Zhang, Parkinson's disease classification using gait analysis via deterministic learning, *Neurosci. Lett.*, **633** (2016), 268–278. https://doi.org/10.1016/j.neulet.2016.09.043
58. F. M. J. Pfister, T. T. Um, D. C. Pichler, J. Goschenhofer, K. Abedinpour, M. Lang, et al., High-resolution motor state detection in Parkinson's disease using convolutional neural networks, *Sci. Rep.*, **10** (2020), 5860. https://doi.org/10.1038/s41598-020-61789-3
59. R. T. White, *Classifying Parkinson's disease through image analysis: Part 2*, Towards Data Science. Available form: https://towardsdatascience.com/classifying-parkinsons-disease-through-image-analysis-part-2-ddbbf05aac21.
60. *Parkinsons drawing Pytorch lightning CNN*, Kaggle. Available form: https://www.kaggle.com/code/stpeteishii/parkinsons-drawing-pytorch-lightning-cnn.
61. M. Shaban, Deep convolutional neural network for Parkinson's disease based handwriting screening, *2020 IEEE 17th International Symposium on Biomedical Imaging Workshops (ISBI Workshops)*, 2020, 1–4. https://doi.org/10.1109/ISBIWorkshops50223.2020.9153407

62. *Detecting Parkinson's disease with OpenCV, computer vision, and the spiral/wave test*, Adrian Rosebrock, April 29, 2019. Available form: https://pyimagesearch.com/2019/04/29/detecting-parkinsons-disease-with-opencv-computer-vision-and-the-spiral-wave-test/.
63. P. Zham, D. K. Kumar, P. Dabnichki, S. Poosapadi Arjunan, S. Raghav, Distinguishing different stages of Parkinson's disease using composite index of speed and pen-pressure of sketching a spiral, *Front Neurol.*, **8** (2017), 435. https://doi.org/10.3389/fneur.2017.00435
64. J. B. Liu, N. Salamat, M. Kamran, S. Ashraf, R. H. Khan, Single-valued neutrosophic set with quaternion information: a promising approach to assess image quality, *Fractals*, **31** (2023), 1–10. https://doi.org/10.1142/S0218348X23400741
65. J. B. Liu, X. B. Peng, J. Zhao, Analyzing the spatial association of household consumption carbon emission structure based on social network, *J. Comb. Optim.*, **45** (2023), 79. https://doi.org/10.1007/s10878-023-01004-x
66. J. B. Liu, Y. Bao, W. T. Zheng, S. Hayat, Network coherence analysis on a family of nested weighted *n*-polygon networks, *Fractals*, **29** (2021), 2150260. https://doi.org/10.1142/S0218348X21502601

AIMS Press

© 2024 the Author(s), licensee AIMS Press. This is an open access article distributed under the terms of the Creative Commons Attribution License (http://creativecommons.org/licenses/by/4.0)